ACS APPLIED MATERIALS & INTERFACES

Research Article

www.acsami.org

Conjugated Phosphonic Acid Modified Zinc Oxide Electron Transport Layers for Improved Performance in Organic Solar Cells

Jennifer L. Braid,[†,‡] Unsal Koldemir,[§] Alan Sellinger,*[,‡,§] Reuben T. Collins,*[,†] Thomas E. Furtak,[†] and Dana C. Olson*[,‡]

[†]Department of Physics and [§]Department of Chemistry and Geochemistry, Colorado School of Mines, Golden, Colorado 80401, United States

[‡]National Renewable Energy Laboratory, Golden, Colorado 80401, United States

ABSTRACT: Phosphonic acid modification of zinc oxide (ZnO) electron transport layers in inverted P3HT:ICBA solar cells was studied to determine the effect of conjugated linkages between the aromatic and phosphonic acid attachment groups. For example, zinc oxide treated with 2,6-difluorophenylvinylphosphonic acid, having a conjugated vinyl group connecting the aromatic moiety to the phosphonic acid group, showed a 0.78 eV decrease in the effective work function versus unmodified ZnO, whereas nonconjugated 2,6-difluorophenylethylphosphonic acid resulted in a 0.57 eV decrease, as measured by Kelvin probe. This resulted in an average power conversion efficiency of 5.89% for conjugated 2,6-difluorophenyvinylphosphonic acid modified solar cells, an improvement over unmodified (5.24%) and nonconjugated phosphonic acid modified devices (5.64%), indicating the importance of the conjugated linkage.

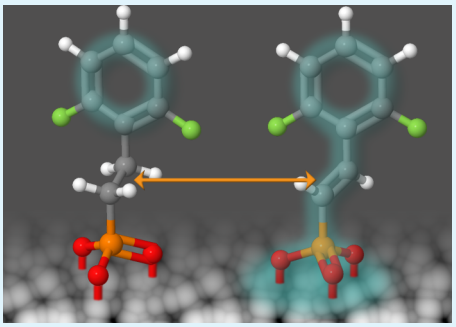

KEYWORDS: *organic photovoltaics, inverted devices, work function tuning, phosphonic acid, conjugated linkage*

INTRODUCTION

Organic photovoltaics are a viable source of scalable, renewable energy because of their potentially low-cost, lightweight, low-temperature, and high-throughput manufacturing. Single-junction power conversion efficiencies have recently reached 9.2% for polymer:fullerene cells,[1] with tandem polymer device efficiency having already surpassed 10%.[2] These bulk heterojunction cells can be prepared by two architectures, namely traditional and inverted. The traditional architecture in an organic solar cell generally uses PEDOT:PSS as a hole transport layer with a transparent electrode, indium tin oxide (ITO), that collects the holes. Inverted devices, on the other hand, use an electron transport layer, such as ZnO, thereby employing ITO to collect electrons. As such, the inverted device architecture avoids stability problems associated with both the PEDOT:PSS/ITO interface, as well as diffusion of water and oxygen into the low work function anode, usually Al or Ca/Al for traditional devices.[3] Thus, inverted devices have led to increased device stability and performance and therefore longer lifetimes, especially with the introduction of ZnO as a charge-selective interlayer.[4,5]

As an electron transport layer, ZnO has been commonly used due to its electron selectivity, ease of thin film formation by a variety of deposition methods, high electron mobility, good transparency, earth abundance, and low cost.[6−11] It is worth noting that any mismatch between the Fermi level of ZnO and the electron transport level of the active layer may result in energy loss during charge extraction.[11,12] Because of this energy loss, quasi-Fermi level matching between the active layer and the charge transport layers has become an important attribute in maximizing efficiency in organic hybrid photovoltaics. Adjusting the alignment of the effective work function of charge transport layers to the charge transport levels of the active layer has been shown to influence the efficiency of charge extraction and the open circuit voltage of bulk heterojunction solar cells,[9−15] as well as charge injection in organic light emitting diodes.[16−19]

In this context, a molecular dipolar surface modifier may be used to alter the alignment of the effective work function of ZnO relative to the lowest unoccupied molecular orbital (LUMO) of the electron acceptor material at the BHJ interface, without changing the intrinsic Fermi level or carrier density of the bulk oxide. Better energy alignment at the interface reduces the energy lost during electron extraction/injection, increasing the open circuit voltage, the built-in field, and thereby the fill factor of the device.[9−12,20] The relationship between the work function of the contact and open circuit voltage has also been shown on ITO in standard architecture devices.[14,15]

Changes in the effective work function of a surface modified with a molecular dipole can result from the change in vacuum level and the bond dipole created by the surface bond.[14,21−24] The change in the vacuum level across the monolayer itself is defined to be proportional to the component of the molecular dipole moment perpendicular to the surface. Therefore, the influence of a molecular dipolar surface modifier on effective work function is divided into two contributions: (i) the dipole

Received: August 6, 2014
Accepted: October 20, 2014
Published: October 20, 2014

of the molecular monolayer along the surface normal, and (ii) the interfacial dipole created by charge redistribution due to the surface bond. As molecular dipolar surface modifiers, benzylphosphonic acids have shown promise; effectively increasing or decreasing the work function of various transparent conductive oxides, including ITO,[6,14,15,18,20,23,25,26] GZO,[22] and ZnO,[6,11] by up to 1 eV depending on the orientation and strength of the molecular dipole. Recently, benzylphosphonic acids with various head groups, and therefore different dipole moments, have been used to alter the work function of the modified oxide by shifting the vacuum level of the oxide (i), whereas the bond dipole (ii) remains relatively constant.[11,14,15,20,25]

Orthodifluorobenzylphosphonic acid (oF_2BPA), which has been investigated previously,[7,8,11,14,15,20,22,23,25] decreases the work function of zinc oxide, and is shown to increase the open circuit voltage in inverted architecture devices.[11] In this study, we introduce two small polar phosphonic acids with the same attachment and head groups as oF_2BPA, but different linkages connecting the two moieties (Figure 1). Specifically, we utilize a conjugated trans double bond as a linker between the aromatic ring and the phosphonic acid group in 2,6-orthodifluorophenylvinylphosphonic acid (oF_2PVPA), and compare it with the nonconjugated orthodifluorophenylethylphosphonic acid (oF_2PEPA), having a saturated ethyl linkage. These molecules, having similar lengths and molecular dipole moments should therefore have similar effects on the vacuum level of ZnO. However, the different linkages may allow for variation in the bond dipole through direct conjugation with the acid binding group.

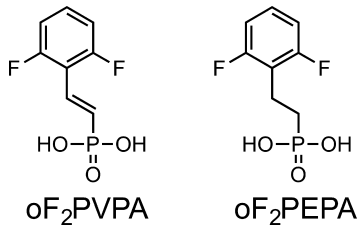

Figure 1. Two phosphonic acids used in this study: orthodifluorophenylethylphosphonic acid (oF_2PEPA), and orthodifluorophenylvinylphosphonic acid (oF_2PVPA).

A double bond between two carbon atoms allows for delocalization of the associated π-electrons of the aromatic ring into the phosphonic acid attachment group, potentially facilitating a change in the molecular dipole as well as improved charge transport between the molecule and the oxide. We hypothesized that the introduction of the conjugated double bond would increase the electron charge redistribution at the interface, increase the bond dipole, and accentuate the shift in work function. Our results show the conjugated oF_2PVPA does outperform the nonconjugated analogue, oF_2PEPA, in modification of the effective work function of zinc oxide by 0.21 mV. The conjugated linkage led not only to an improvement in work function, but also to increased open circuit voltage, short circuit current, and power conversion efficiency (PCE) of devices compared to the nonconjugated modifier. Overall the PCE was increased by over 12% versus the unmodified ZnO interface (5.89 vs 5.24%). Infrared spectroscopic characterization of these phosphonic acids on ZnO indicates that they bind in a bidentate and/or tridentate fashion, with similar surface coverage.

RESULTS AND DISCUSSION

Synthesis of oF_2PEPA, oF_2PVPA. The conjugated orthodifluorophenylvinylphosphonic acid (oF_2PVPA) and nonconjugated orthodifluorophenylethylphosphonic acid (oF_2PEPA) were synthesized as shown in Scheme 1, with all synthetic details outlined in the Experimental Methods section. Preparation of oF_2PVPA was achieved via Heck coupling between 2,6-difluoroiodobenzene (1) and diethyl vinylphosphonate using Herrmann's palladacycle in 66% yield. As Heck coupling is more prevalent for styrenyl and acrylate based systems, performing this on vinylphosphonates is not very common and required careful experimental optimization. The intermediate vinyl bridged compound (2) was used to prepare both the oF_2PVPA and oF_2PEPA. The oF_2PVPA was prepared via deprotection of the vinyl bridged phosphonic ester using a combination of trimethylsilyl bromide/potassium iodide (TMSBr/KI) in acetonitrile (ACN). In the case of oF_2PEPA, the vinyl group was hydrogenated using triethyl silane (TES) as a hydrogen source over Pd/C catalyst under mild conditions to afford the ester precursor (3) in 67% yield. The desired oF_2PVPA and oF_2PEPA phosphonic acid products were obtained in 48 and 42% yield, respectively.

Scheme 1. Synthetic Preparation of the Conjugated Orthodifluorophenylvinylphosphonic Acid (oF_2PVPA) and Nonconjugated Orthodifluorophenylethylphosphonic acid (oF_2PEPA)

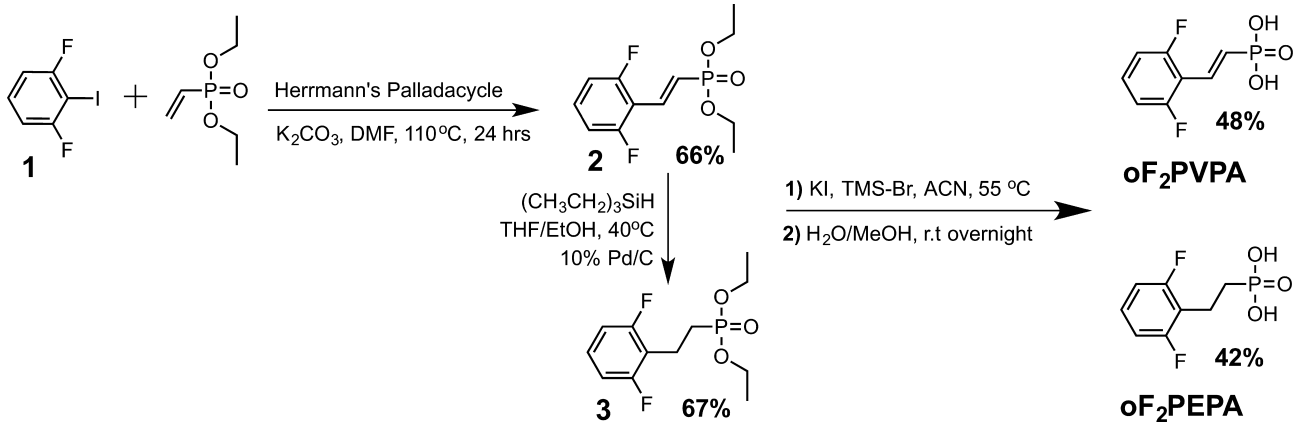

dx.doi.org/10.1021/am505182c | ACS Appl. Mater. Interfaces 2014, 6, 19229–19234

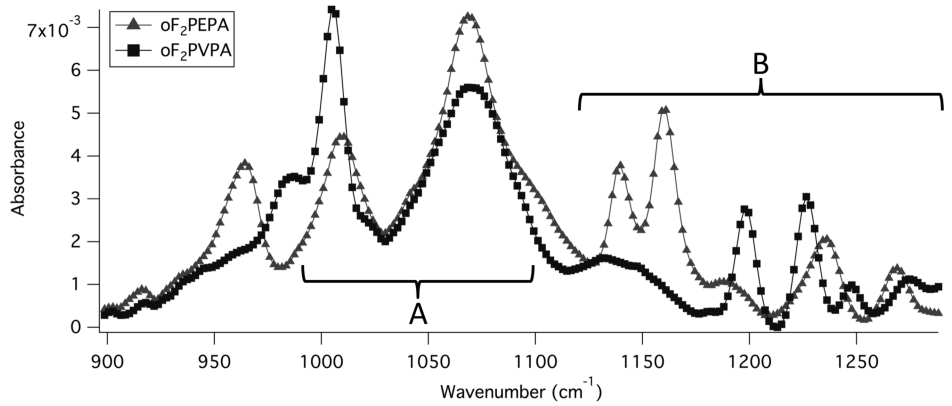

Figure 2. FTIR spectra for oF_2PEPA and oF_2PVPA bonded to ZnO. Region A, 990−1100 cm^{-1}, contains stretching modes of PO_3^{2-}. Region B, 1125−1300 cm^{-1}, shows P−O−Zn and P═O−Zn vibrations, and may exhibit free P═O signatures for both molecules.

Table 1. Work Function (KP Measurements) of PA-Modified ZnO and Corresponding Average Device Results

	$\Delta\phi$ (eV)	V_{OC}(V)	J_{SC}(mA/cm^2)	FF (%)	PCE (%)	R_{SH} (kΩ)	R_{SE} (Ω)
ZnO		0.74 ± 0.01	10.19 ± 0.13	69.1 ± 0.8	5.24 ± 0.05	158 ± 2	18.7 ± 0.1
oF_2PEPA	0.57 ± 0.01	0.76 ± 0.01	10.35 ± 0.14	71.7 ± 0.2	5.64 ± 0.09	369 ± 7	17.7 ± 0.1
oF_2PVPA	0.78 ± 0.01	0.78 ± 0.01	10.55 ± 0.12	71.6 ± 0.3	5.89 ± 0.04	344 ± 4	20.3 ± 0.3

Binding Characteristics on Zinc Oxide. The oF_2PVPA and oF_2PEPA are spin-cast via ethanol solutions onto zinc oxide that had been deposited from a dilute solution of diethylzinc in a toluene/tetrahydrofuran solvent mixture. After spin-casting, the films are annealed at 120 °C and rinsed with ethanol to ensure monolayer or submonolayer coverage of the respective phosphonic acids. Next, we performed Fourier transform infrared spectroscopy (FTIR) to identify the vibrational fingerprints of these molecules bonded to zinc oxide, which allows us to verify attachment as well as compare the surface coverage and binding configurations of these modifiers.

As may be seen in Figure 2, the region of 900−1300 cm^{-1} contains several characteristic vibrations of the P═O and P−O−(H) terminations. Because of similar feature sizes across the FTIR spectra, we infer that the surface coverage is roughly equal for both molecules. The peaks at ∼1000 and 1070 cm^{-1} for both oF_2PEPA and oF_2PVPA, shown in region A, are associated with symmetric and asymmetric P−O stretching in PO_3^{2-}, respectively.[27,28] This indicates fully deprotonated phosphonic acids, bonded to Zn sites with both P−O-(H) ligaments. The lack of features at 925 and 940 cm^{-1}, normally attributed to P−O−H stretching,[29] points to few or no unattached P−O−H ligaments. Also absent is a large band centered at 1230 cm^{-1}, which would signify unbound P═O terminations.[7] Instead, we find smaller features in 1130−1300 cm^{-1}, labeled region B. Peaks in this region could represent $\nu(PO_2^-)$ stretching vibrations associated with one bound and one free P−O−H ligament,[28] though we should also see free P−O−H signatures at 925 and 940 cm^{-1} with this mode. Therefore, we suspect that the peaks between 1130 and 1300 cm^{-1} are P−O−Zn and P═O−Zn vibrations, expected between 1160 and 1230 cm^{-1}.[28] Because these modes are known to shift with electron affinity, we credit the variation in peak position to the change in linkage between these molecules, because of delocalization of the π-electrons of the aromatic ring. Specifically, we suspect the pair of peaks in the oF_2PEPA spectrum at 1140 and 1160 cm^{-1} is shifted to higher energies (1200 and 1225 cm^{-1}) for oF_2PVPA due to the conjugation. However, some of the features in region B could belong to unbound P═O ligaments,[30] shifted by P−O−(H) terminations binding to Zn sites and different linkages within the phosphonic acids, suggesting the possibility of some unbound P═O terminations. We conclude that both oF_2PVPA and oF_2PEPA bind to ZnO via multidentate attachment, most likely a mixture of bidentate and tridentate configurations.

Work Function Modification and Device Results. After confirming the attachment of these phosphonic acids on zinc oxide, work function measurements of treated and untreated zinc oxide were performed with a Kelvin probe setup at ambient conditions to determine the extent of change in work function as shown in Table 1. We observed a large shift in the effective work function of zinc oxide when modified with each phosphonic acid, with conjugated oF_2PVPA decreasing the work function by 0.78 eV, a 0.21 eV greater change versus the similarly sized oF_2PEPA. We attribute the enhanced shift in work function for zinc oxide modified with oF_2PVPA over oF_2PEPA to better charge delocalization between oF_2PVPA and ZnO via the π-electrons of the conjugated linkage.

Changing the linkage within our phosphonic acid would have some effect on the intrinsic dipole moment of the molecule, but it may also alter the bond dipole created at the phosphonic acid/oxide interface. We see a larger change in the work function of ZnO modified with oF_2PVPA versus oF_2PEPA, which lacks conjugation in its linkage. The conjugation likely improves the change in work function in two ways: (i) a larger molecular dipole moment, and (ii) a larger bond dipole contribution, both resulting from the delocalized π-electrons in the aromatic ring having better communication with the bonding phosphonic acid through the vinyl linkage.

Finally, inverted architecture devices were fabricated on ITO-patterned glass substrates. The ZnO electron transport layer was deposited from the diethylzinc solution, onto which phosphonic acid modifiers were spin-cast. These films were then annealed at 120 °C to promote binding, and rinsed with ethanol to remove unbound species and promote monolayer coverage of phosphonic acids. P3HT:ICBA bulk heterojunction active layers were subsequently spin-cast and slow-dried,

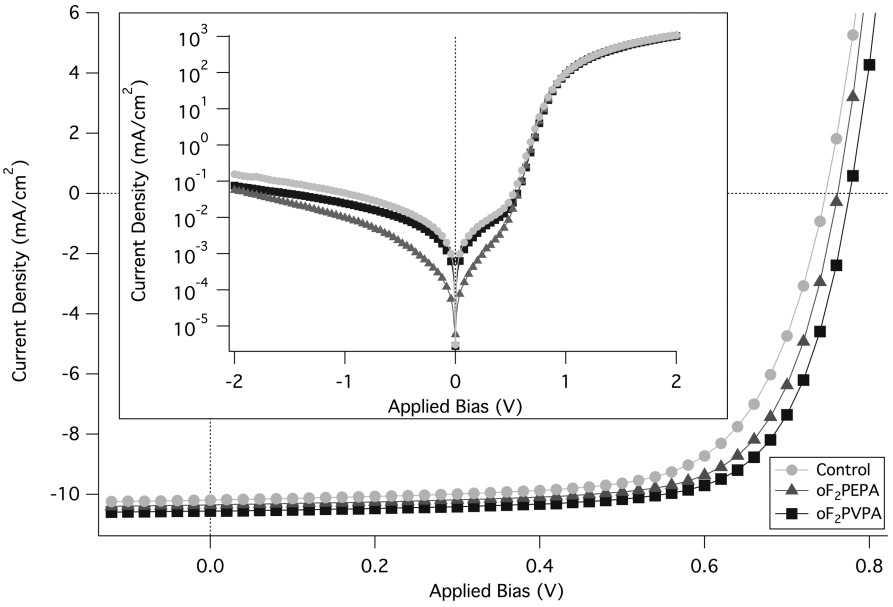

Figure 3. Average $J-V$ characteristics for PA-modified ZnO devices under illumination. The inset shows average $J-V$ characteristics in the dark on a semilog scale (corresponding parameters in Table 1).

followed by thermal evaporation of the MoO_3 hole transport layer and the Ag cathode. The solar cell device parameters are summarized in Table 1, and $J-V$ curves are presented in Figure 3. At first glance, we observe a systematic increase in the open circuit voltage that is due to the decrease in effective work function for oF_2PEPA and oF_2PVPA-modified ZnO. The subunity relation between change in V_{OC} and work function shift has been previously attributed to Fermi-level pinning as the oxide work function approaches the LUMO level of the BHJ.[10,17,31,32]

The short circuit current was also improved for oF_2PVPA versus the control device and nonconjugated oF_2PEPA. This agrees with the prediction of improved energy level alignment at the BHJ/ETL interface and a resulting increase in the electron transfer rate. The boost in fill factor from 69.1% for the unmodified device to 71.7% for oF_2PEPA and 71.6% for oF_2PVPA is the result of reduced recombination associated with the change in effective work function of the ZnO contact and a corresponding increase in the electric field across the active layer. Additionally, the shunt resistance (R_{SH}) is improved with modification by both oF_2PEPA and oF_2PVPA, signifying that these modifiers may inhibit leakage current in reverse bias. Because low R_{SH} can result in a decrease in V_{OC}, the effect of these modifiers on leakage current may also be contributing to the improved open circuit voltage of the PA-modified devices. However, the modifiers also increase the series resistance (R_{SE}) of the device, which may explain why fill factor did not further improve for the oF_2PVPA modified device.

CONCLUSIONS

Zinc oxide modified with 2,6-difluorophenylvinylphosphonic acid (oF_2PVPA) measured with Kelvin probe showed a 0.78 eV decrease in the effective work function compared to unmodified ZnO, while nonconjugated 2,6-difluorophenylethylphosphonic acid (oF_2PEPA) decreased the effective work function of ZnO by only 0.57 eV. Inverted P3HT:ICBA solar cells modified with the conjugated oF_2PVPA improved both open circuit voltage and power conversion efficiency over oF_2PEPA, and showed a 40 mV boost in open circuit voltage and increased power conversion efficiency over unmodified solar cells. Through FTIR characterization, the attachment of these molecules was found to be predominantly bidentate/tridentate to ZnO, and the conjugated linkage is shown to affect binding energy. That this conjugated linkage dramatically accentuates the effect of the molecule on the work function of the modified surface shows it to be an interesting approach in improving quasi-Fermi level alignment in organic photovoltaics. An important finding was that the open circuit voltage of modified devices was shifted by a much smaller, but dependent amount to the change in work function, as is common in this type of device. Furthermore, the simple synthesis of conjugated molecules from commercially available precursors makes this type of linkage extremely viable for continued study with other types dipolar molecules on various contact surfaces for use in organic hybrid electronics.

EXPERIMENTAL METHODS

Synthesis of oF_2PVPA, oF_2PEPA. *Diethyl (E)-(2,6-difluorostyryl)phosphonate (oF_2PVPA):*[33] A 100 mL Schlenk flask was charged with the aromatic halide (1 equiv.), diethyl vinyl phosphonate (1 equiv.) Herrmann's catalyst (2 mol %) potassium carbonate (1 equiv.) and 20 mL of anhydrous dimethylformamide. The reaction mixture was heated to 110 °C for 24 h under argon. After cooling to room temperature, water (100 mL) was added and the mixture was stirred for 30 min. The organic layers were extracted with dichloromethane (100 mL) three times and dried over magnesium sulfate. Then, the solvent was evaporated under vacuum resulting in the yellow oil crude product. The product was obtained after purification by column chromatography eluting with petroleum ether: ethyl acetate (1:1). Start with 1g (4.16 mmol) of 1,3-difluoro-2-iodobenzene. The product was obtained 0.76 g (66%) of a yellow oil. ^{1}H NMR (500 MHz, $CDCl_3$): δ = 7.48−7.57 (dd, 1H, J = 20 Hz), 7.24−7.31 (m, 1H), 6.88−6.92 (m, 2H), 6.59 (t, 1H, J = 20 Hz), 4.12 (t, 4H, J = 10 Hz), 1.31−1.35 (m, 6H). ^{13}C NMR (125 MHz, $CDCl_3$) δ = 162.53, 160.56, 134.81, 131.20, 129.19, 120.70, 111.99, 111.78, 62.02, 16.43.

Diethyl (2,6-Difluorophenethyl)phosphonate (oF_2PEPE).[34] A 100 mL oven-dried Schlenk flask was charged with diethyl (E)-(2,6-difluorostyryl)phosphonate (0.9 g, 3.25 mmol), 10% Pd/C (0.11 mg),

anhydrous THF (15 mL) and anhydrous ethanol (2 mL). To this mixture, triethylsilane (3.78 g, 5.22 mL, 32.5 mmol) was added dropwise. After bubbling was quenched, the reaction was heated to 40 °C for 4 h. After cooling to room temperature, solvents were evaporated under vacuum. The resulting crude was suspended in DCM (50 mL) and filtered through a plug of Celite. After evaporating the volatiles, the product was obtained 0.6 g (67%) of a colorless oil. ^{1}H NMR (500 MHz, $CDCl_3$): δ = 7.02−7.13 (m, 1H), 6.75−6.80 (m, 2H), 4.00−4.07 (m, 4H), 2.85−2.89 (m, 2H), 1.92−1.98 (m, 2H), 1.21−1.27 (m, 3H) ^{13}C NMR (125 MHz, $CDCl_3$) δ = 162,34, 160.38, 128.04, 116.73, 111.27, 111.06, 61.71, 61.65, 25.90, 24.79, 16.41, 16.36.

General Reaction Protocol for the Synthesis of Vinylphosphonic Acids.[23] A 100 mL two neck flask equipped with a condenser and a stir bar was charged with the phosphonic ester (1 equiv.), potassium iodide (3 equiv.), and 20 mL of anhydrous acetonitrile. The mixture was cooled to 0 °C and then bromotrimethylsilane (3 equiv) was added dropwise. Ice−water bath was removed and the reaction mixture was heated to 55 °C for 6 h under argon forming pink color with white precipitates. Next, the reaction mixture was cooled down to room temperature and the volatiles were removed under vacuo yielding a brown solid. Then, 50 mL of methanol:water (1:1) solution was added and the reaction mixture was stirred at room temperature overnight. After cooling to room temperature, the solvents were evaporated under vacuum yielding crude product as brown solid. The respective products were obtained by recrystallization as white powders

(E)-(2,6-difluorostyryl)phosphonic acid (oF$_2$PVPA). Start with 0.74 g (2.83 mmol) diethyl (E)-(2,6-difluorostyryl)phosphonate. The product was obtained 0.30 g (48%) of a white powder after recrystallization from acetonitrile. ^{1}H NMR (500 MHz, DMSO-d_6): δ = 7.43−7.51 (m, 1H), 7.15−7.23 (m, 3H), 6.57 (t, 1H, J = 15 Hz). ^{13}C NMR (125 MHz, DMSO-d_6) δ = 161.58, 159.57, 131.41, 129.00, 128.62, 127.58, 112.41, 112.21.

(2,6-Difluorophenethyl)phosphonic Acid (oF$_2$PEPA). Start with 0.6 g (2.16 mmol) diethyl (2,6-difluorophenethyl)phosphonate. The product was obtained 0.20 g (42%) of a white powder after recrystallization from acetonitrile. ^{1}H NMR (500 MHz, DMSO-d_6): δ = 7.27−7.33 (m, 1H), 7.02−7.09 (m, 2H), 3.99 (s, br, -POOH), 2.78−2.83 (m, 2H), 1.69−1.76 (m, 2H) ^{13}C NMR (125 MHz, DMSO-d_6) δ = 161.86, 159.91, 128.71, 117.24, 111.81, 111.61, 27.41, 16.32.

Fourier-Transform Infrared Spectroscopy. Polished silicon wafers (525 μm thick) are cut into 1" squares, which are then cleaned and prepared with ZnO and PA films using the same procedure for glass/ITO substrates for devices, including the subsequent rinse and annealing steps. FTIR spectroscopy was completed using a Thermo Scientific Nicolet 6700 FT-IR Spectrometer with a liquid nitrogen cooled Hg−Cd−Te detector and KBr beam splitter. Normal-incidence transmission measurements were completed for thin films of PAs on ZnO on Si.

Kelvin Probe Measurements. Glass/ITO substrates are cleaned and prepared with ZnO and PA films as for devices, including the subsequent rinse and annealing steps. A KPTechnology SKP/SVP/LE 450 system is utilized for Kelvin probe measurements of the work function and calibrated with Al and Au reference samples in air. All work function measurements are then calculated as change from the ZnO control.

Device Fabrication. Devices were fabricated on 1 in. × 1 in. glass substrates with patterned ITO (Thin Film Devices), with better than 84% optical transparency and sheet resistance of approximately 10 Ω/□. The substrates are cleaned by sonicating first in acetone, then isopropanol, for 15 min each. Next, they are treated with a Jelight Company, Inc. model 42 UV−O_3 cleaner for 15 min and used immediately afterward. Zinc oxide is deposited from a solution prepared in an inert environment from a 1.1 M diethyl zinc precursor (Sigma-Aldrich) in toluene mixed (1:2 by volume) with anhydrous tetrahydrofuran (Sigma-Aldrich). The zinc oxide film is spin-cast in air at 6000 rpm for 60s, followed by annealing in air at 120 °C for 10 min.

Ten millimolar ethanol solutions of oF$_2$PEPA and oF$_2$PVPA are prepared and spin-cast in air at 2000 rpm for 60s. The samples are then annealed in air at 120 °C for 10 min, rinsed with ethanol, blown dry with nitrogen, and annealed again at 120 °C for 5 min.

The active layer solution is prepared with equal weights of P3HT (BASF) and ICBA (Plextronics), for total solids of 34 mg/mL in 1,2-dichlorobenzene. The solution is stirred overnight at 60 °C. The bulk heterojunction is spin-cast in an inert (N_2) environment at 800 rpm for 30 s. The samples are allowed to dry for several hours in covered Petri dishes, and then annealed at 155 °C for 10 min in the nitrogen environment.

Molybdenum oxide (Strem Chemicals) is thermally evaporated at a rate of 0.1 Å/s, followed by the Ag cathode at 0.5 Å/s, with base pressure below 1 × 10^{-7} Torr.

Device Characterization. Devices were tested using a solar simulator with a quartz halogen lamp (1.1 spectral mismatch factor as compared with the solar spectrum for PCDTBT:PC_{71}BM) in an inert (N_2) environment. A 0.06 cm^2 aperture was used to avoid edge effects. A voltage bias was applied via the ITO and Ag electrodes and the resulting current density was measured. Series resistance was measured at 1.2 V applied bias.

AUTHOR INFORMATION

Corresponding Authors

*E-mail: dana.olson@nrel.gov.
*E-mail: aselli@mines.edu.
*E-mail: rtcollin@mines.edu.

Notes

The authors declare no competing financial interest.

ACKNOWLEDGMENTS

This work was supported by the U.S. Department of Energy under Contract DE-AC36−08-GO28308 with the National Renewable Energy Laboratory through the DOE SETP program. Partial support from the National Science Foundation through Grant DMR-0907409 and the Renewable Energy Materials Research Science and Engineering Center is also acknowledged for RTC and TEF.

REFERENCES

(1) He, Z.; Zhong, C.; Su, S.; Xu, M.; Wu, H.; Cao, Y. Enhanced Power-Conversion Efficiency in Polymersolar Cells Using an Inverted Device Structure. *Nat. Photonics* **2012**, *6*, 591−595.

(2) You, J.; Dou, L.; Yoshimura, K.; Kato, T.; Ohya, K.; Moriarty, T.; Emery, K.; Chen, C.-C.; Gao, J.; Li, G.; Yang, Y. A Polymer Tandem Solar Cell with 10.6% Power Conversion Efficiency. *Nat. Commun.* **2013**, *4*, 1446−10.

(3) White, M. S.; Olson, D. C.; Shaheen, S. E.; Kopidakis, N.; Ginley, D. S. Inverted Bulk-Heterojunction Organic Photovoltaic Device Using a Solution-Derived ZnO Underlayer. *Appl. Phys. Lett.* **2006**, *89*, 143517.

(4) Kyaw, A. K. K.; Sun, X. W.; Jiang, C. Y.; Lo, G. Q.; Zhao, D. W.; Kwong, D. L. An Inverted Organic Solar Cell Employing a Sol−Gel Derived ZnO Electron Selective Layer and Thermal Evaporated MoO_3 Hole Selective Layer. *Appl. Phys. Lett.* **2008**, *93*, 221107.

(5) Lloyd, M. T.; Peters, C. H.; Garcia, A.; Kauvar, I. V.; Berry, J. J.; Reese, M. O.; McGehee, M. D.; Ginley, D. S.; Olson, D. C. Influence of Hole-Transport Layer on the Initial Behavior and Lifetime of Inverted Organic Photovoltaics. *Sol. Energy Mater. Sol. Cells* **2011**, *95*, 1382−1388.

(6) Bulusu, A.; Paniagua, S. A.; MacLeod, B. A.; Sigdel, A. K.; Berry, J. J.; Olson, D. C.; Marder, S. R.; Graham, S. Efficient Modification of Metal Oxide Surfaces with Phosphonic Acids by Spray Coating. *Langmuir* **2013**, *29*, 3935−3942.

(7) Hotchkiss, P. J.; Malicki, M.; Giordano, A. J.; Armstrong, N. R.; Marder, S. R. Characterization of Phosphonic Acid Binding to Zinc Oxide. *J. Mater. Chem.* **2011**, *21*, 3107.

(8) Wood, C.; Li, H.; Winget, P.; Bredas, J.-L. Binding Modes of Fluorinated Benzylphosphonic Acids on the Polar ZnO Surface and Impact on Work Function. *J. Phys. Chem. C* **2012**, *116*, 19125−19133.
(9) Ha, Y. E.; Jo, M. Y.; Park, J.; Kang, Y.-C.; Yoo, S. I.; Kim, J. H. Inverted Type Polymer Solar Cells with Self-Assembled Monolayer Treated ZnO. *J. Phys. Chem. C* **2013**, *117*, 2646−2652.
(10) Brenner, T. M.; Chen, G.; Meinig, E. P.; Baker, D. J.; Olson, D. C.; Collins, R. T.; Furtak, T. E. Tuning Zinc Oxide/Organic Energy Level Alignment Using Mixed Triethoxysilane Monolayers. *J. Mater. Chem. C* **2013**, *1*, 5935.
(11) Cowan, S. R.; Schulz, P.; Giordano, A. J.; Garcia, A.; MacLeod, B. A.; Marder, S. R.; Kahn, A.; Ginley, D. S.; Ratcliff, E. L.; Olson, D. C. Chemically Controlled Reversible and Irreversible Extraction Barriers via Stable Interface Modification of Zinc Oxide Electron Collection Layer in Polycarbazole-Based Organic Solar Cells. *Adv. Funct. Mater.* **2014**, *24*, 4671−4680.
(12) MacLeod, B. A.; Schulz, P.; Cowan, S. R.; Garcia, A.; Ginley, D. S.; Kahn, A.; Olson, D. C. Improved Performance in Bulk Heterojunction Organic Solar Cells with a Sol-Gel MgZnO Electron-Collecting Layer. *Adv. Energy Mater.* **2014**, *4*, 1400073.
(13) Kim, J. S.; Park, J. H.; Lee, J. H.; Jo, J.; Kim, D.-Y.; Cho, K. Control of the Electrode Work Function and Active Layer Morphology via Surface Modification of Indium Tin Oxide for High Efficiency Organic Photovoltaics. *Appl. Phys. Lett.* **2007**, *91*, 112111.
(14) Ratcliff, E. L.; Garcia, A.; Paniagua, S. A.; Cowan, S. R.; Giordano, A. J.; Ginley, D. S.; Marder, S. R.; Berry, J. J.; Olson, D. C. Investigating the Influence of Interfacial Contact Properties on Open Circuit Voltages in Organic Photovoltaic Performance: Work Function Versus Selectivity. *Adv. Energy Mater.* **2013**, *3*, 647−656.
(15) Knesting, K. M.; Ju, H.; Schlenker, C. W.; Giordano, A. J.; Garcia, A.; Smith, O. L.; Olson, D. C.; Marder, S. R.; Ginger, D. S. ITO Interface Modifiers Can Improve VOCin Polymer Solar Cells and Suppress Surface Recombination. *J. Phys. Chem. Lett.* **2013**, *4*, 4038−4044.
(16) Hanson, E. L.; Guo, J.; Koch, N.; Schwartz, J.; Bernasek, S. L. Advanced Surface Modification of Indium Tin Oxide for Improved Charge Injection in Organic Devices. *J. Am. Chem. Soc.* **2005**, *127*, 10058−10062.
(17) Braun, S.; Salaneck, W. R.; Fahlman, M. Energy-Level Alignment at Organic/Metal and Organic/Organic Interfaces. *Adv. Mater.* **2009**, *21*, 1450−1472.
(18) Sharma, A.; Hotchkiss, P. J.; Marder, S. R.; Kippelen, B. Tailoring the Work Function of Indium Tin Oxide Electrodes in Electrophosphorescent Organic Light-Emitting Diodes. *J. Appl. Phys.* **2009**, *105*, 084507.
(19) Zhang, B.; Qin, C.; Niu, X.; Xie, Z.; Cheng, Y.; Wang, L.; Li, X. On the Origin of Efficient Electron Injection at Phosphonate-Functionalized Polyfluorene/Aluminum Interface in Efficient Polymer Light-Emitting Diodes. *Appl. Phys. Lett.* **2010**, *97*, 043506.
(20) MacLeod, B. A.; Horwitz, N. E.; Ratcliff, E. L.; Jenkins, J. L.; Armstrong, N. R.; Giordano, A. J.; Hotchkiss, P. J.; Marder, S. R.; Campbell, C. T.; Ginger, D. S. Built-in Potential in Conjugated Polymer Diodes with Changing Anode Work Function: Interfacial States and Deviation From the Schottky−Mott Limit. *J. Phys. Chem. Lett.* **2012**, *3*, 1202−1207.
(21) Li, H.; Paramonov, P.; Bredas, J.-L. Theoretical Study of the Surface Modification of Indium Tin Oxide with Trifluorophenyl Phosphonic Acid Molecules: Impact of Coverage Density and Binding Geometry. *J. Mater. Chem.* **2010**, *20*, 2630.
(22) Li, H.; Ratcliff, E. L.; Sigdel, A. K.; Giordano, A. J.; Marder, S. R.; Berry, J. J.; Bredas, J.-L. Modification of the Gallium-Doped Zinc Oxide Surface with Self-Assembled Monolayers of Phosphonic Acids: a Joint Theoretical and Experimental Study. *Adv. Funct. Mater.* **2014**, *24*, 3593−3603.
(23) Hotchkiss, P. J.; Li, H.; Paramonov, P. B.; Paniagua, S. A.; Jones, S. C.; Armstrong, N. R.; BrÃ das, J.-L.; Marder, S. R. Modification of the Surface Properties of Indium Tin Oxide with Benzylphosphonic Acids: a Joint Experimental and Theoretical Study. *Adv. Mater.* **2009**, *21*, 4496−4501.
(24) Heimel, G.; Romaner, L.; Zojer, E.; Bredas, J.-L. Toward Control of the Metal−Organic Interfacial Electronic Structure in Molecular Electronics: a First-Principles Study on Self-Assembled Monolayers of Π-Conjugated Molecules on Noble Metals. *Nano Lett.* **2007**, *7*, 932−940.
(25) Hotchkiss, P. J.; Jones, S. C.; Paniagua, S. A.; Sharma, A.; Kippelen, B.; Armstrong, N. R.; Marder, S. R. The Modification of Indium Tin Oxide with Phosphonic Acids: Mechanism of Binding, Tuning of Surface Properties, and Potential for Use in Organic Electronic Applications. *Acc. Chem. Res.* **2012**, *45*, 337−346.
(26) Sharma, A.; Haldi, A.; Hotchkiss, P. J.; Marder, S. R.; Kippelen, B. Effect of Phosphonic Acid Surface Modifiers on the Work Function of Indium Tin Oxide and on the Charge Injection Barrier Into Organic Single-Layer Diodes. *J. Appl. Phys.* **2009**, *105*, 074511.
(27) Gliboff, M.; Sang, L.; Knesting, K. M.; Schalnat, M. C.; Mudalige, A.; Ratcliff, E. L.; Li, H.; Sigdel, A. K.; Giordano, A. J.; Berry, J. J.; Nordlund, D.; Seidler, G. T.; Bredas, J.-L.; Marder, S. R.; Pemberton, J. E.; Ginger, D. S. Orientation of Phenylphosphonic Acid Self-Assembled Monolayers on a Transparent Conductive Oxide: a Combined NEXAFS, PM-IRRAS, and DFT Study. *Langmuir* **2013**, *29*, 2166−2174.
(28) Thomas, L. C. *Interpretation of the Infrared Spectra of Organophosphorus Compounds*, 1st ed; Heyden: London, 1974.
(29) Paniagua, S. A.; Hotchkiss, P. J.; Jones, S. C.; Marder, S. R.; Mudalige, A.; Marrikar, F. S.; Pemberton, J. E.; Armstrong, N. R. Phosphonic Acid Modification of Indium−Tin Oxide Electrodes: Combined XPS/UPS/Contact Angle Studies. *J. Phys. Chem. C* **2008**, *112*, 7809−7817.
(30) Zhang, B.; Kong, T.; Xu, W.; Su, R.; Gao, Y.; Cheng, G. Surface Functionalization of Zinc Oxide by Carboxyalkylphosphonic Acid Self-Assembled Monolayers. *Langmuir* **2010**, *26*, 4514−4522.
(31) Mihailetchi, V. D.; Blom, P. W. M.; Hummelen, J. C.; Rispens, M. T. Cathode Dependence of the Open-Circuit Voltage of Polymer:Fullerene Bulk Heterojunction Solar Cells. *J. Appl. Phys.* **2003**, *94*, 6849.
(32) Greiner, M. T.; Helander, M. G.; Tang, W.-M.; Wang, Z.-B.; Qiu, J.; Lu, Z.-H. Universal Energy-Level Alignment of Molecules on Metal Oxides. *Nat. Mater.* **2011**, *11*, 76−81.
(33) Al-Maksoud, W.; Mesnager, J.; Jaber, F.; Pinel, C.; Djakovitch, L. Synthesis of Diethyl 2-(Aryl)Vinylphosphonates by the Heck Reaction Catalysed by Well-Defined Palladium Complexes. *J. Organomet. Chem.* **2009**, *694*, 3222−3231.
(34) Mandal, P. K.; McMurray, J. S. Pd−C-Induced Catalytic Transfer Hydrogenation with Triethylsilane. *J. Org. Chem.* **2007**, *72*, 6599−6601.